

PET/CT in Non-Small-Cell Lung Cancer: Value of Respiratory-Gated PET

Steven M. Larson; Sadek A. Nehmeh; Yusuf E. Erdi; John L. Humm

The use of PET in the staging of patients with NSCLC is cost-effective, mainly due to a reduction in the number of futile operations. The addition of SUVmax to pathologic tumor size identifies a subgroup of patients at highest risk for death as a result of recurrent disease after resection. Tumor staging is more accurate with PET-CT than with CT alone or with PET alone. The greatest source of error in accurate localization and quantification on PET or PET-CT in lung cancer is respiratory motion. At MSKCC respiratory-gated PET (RGPET) is used in treatment planning. The lesion in the gated image is smaller in diameter than in the ungated image. Respiratory-correlated dynamic PET (RCDPET) can be considered an alternative method to RGPET. RCDPET shows very accurate local co-registration that can be used to make an attenuation correction and obtain an SUV. Gating gives a much clearer picture resulting in more than a one-third increase in the quantification. The SUV of lung lesions must be re-evaluated based on these techniques. This development will have important implications in areas such as the liver for controlling respiratory motion, which is a major problem in terms of lesion detection. We have successfully taken the first step in an attempt to correct for respiratory motion artifacts in PET imaging of lung lesions. (*Chang Gung Med J* 2005;28:306-14)

Key words: respiratory-gated PET (RGPET), respiratory-correlated dynamic PET (RCDPET), non-small-cell Lung Cancer (NSCLC), fluoro-2-deoxy-D-glucose (FDG).

Nuclear medicine is contributing to a medical revolution in which targeted therapy and better radiotherapy methods are being rapidly developed. As well, refinements in diagnostic imaging are being introduced in order to guide these important therapies.

Positron emission tomography (PET)

The basis for PET is 'the racer principle'. A radioactive form of a biologically important chemical is used to trace the metabolism of the natural form of that chemical through imaging. Fortunately, biologically relevant tracers of many kinds (^{15}O , ^{13}N , ^{11}C , ^{18}F , ^{86}Y , $^{94\text{m}}\text{Tc}$, ^{124}I [all 'positron emitters']) are

available to label nutrients, drugs, vitamins, antibodies, even cellular elements. In the future many new radiopharmaceuticals will be introduced in the clinical area as well as in research.

Tumor staging and monitoring treatment response

PET is used to detect the living chemistry of the tumor by means of biomedical tracers. The most common tracer is a form of glucose (e.g. FDG), which allows us to look at glycolysis, the biochemical process in the tissue. Changes in biochemical signals are used to monitor tumor response (functional imaging). In the USA, PET is well accepted, and it is

From the Memorial Sloan Kettering Cancer Center, USA.

Received: Feb. 22, 2005; Accepted: Feb. 22, 2005

Address for reprints: Dr. Steven M. Larson, Memorial Sloan-Kettering Cancer Center, Nuclear Medicine Service, 1275 York Avenue, New York, NY 10021, USA. Tel.: (212)639-7373; Fax: (212)717-3263

now reimbursed for major cancers by the USA Federal Government under Medicare (CMS reimbursement as of 1 October 2002). These cancers include (1) non-small-cell lung cancer (NSCLC); (2) colorectal cancer; (3) head and neck cancer (excluding thyroid cancer); (4) melanoma; (5) lymphoma; (6) esophageal cancer; and (7) breast cancer. Why is this important? Reimbursement drives the availability of PET for patient care because it has been demonstrated that these tools are useful for patient management and patient care. The tremendous investment being made now in instrumentation, new radiopharmaceuticals, and novel clinical applications is happening only because of major reimbursement.

The impact of PET on patient management include (1) improving proper staging and permits better treatment planning; (2) detecting occult disease to improve chances of cure; (3) defining the need for intervention for critically located disease, thus reducing morbidity; (4) predicting prognosis; (5) helping with radiation treatment planning; and (6) predicting and monitoring treatment response.

Case study of a patient with a solitary pulmonary nodule

A 55-year-old man presented to Memorial Sloan Kettering Cancer Center (MSKCC) for a rib injury on the left side. He had aspirated food and performed a Heimlich maneuver on himself by pressing into a table at the restaurant. He managed to dislodge a chunk of steak, but in so doing, he injured his ribs on the left side. When he went to his doctor, the chest X-ray showed an R/O rib fracture. But, his doctor also noticed a nodule in his lung. When a PET scan was done with a 3-dimensional data set, a hot spot was seen toward the posterior representing a hyper-metabolizing tumor (Fig. 1). An abnormal spot in the bone was also found (Fig. 2). It showed the typical round appearance of metastasis originating in the bone marrow and later involving the bone. So, this patient actually had other metastases. These findings were confirmed by other techniques (e.g. magnetic resonance imaging (MRI), and a biopsy was directed to that site.

Tumor staging before lung surgery

Another important use of PET scanning is in staging before lung surgery. It is important to know whether the lesion has spread to the mediastinum

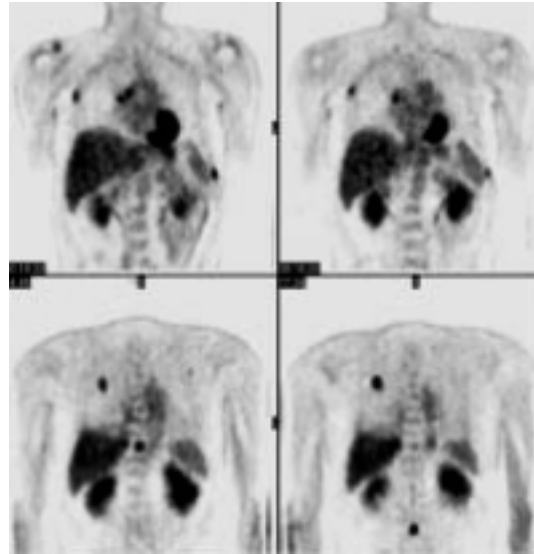


Fig. 1 FFDG-PET 55-year-old man SPN RUL.

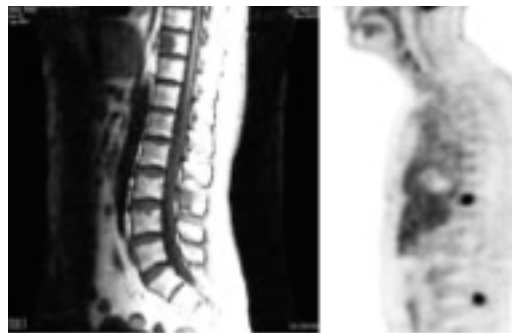


Fig. 2 FDG-PET: Sagittal view of the spine.

because it can complicate surgery. Figure 3 shows the extent of the tumor in a patient with Stage IIIA lung cancer. This patient had a primary tumor but also involvement of the lymph nodes. The primary tumor spread to the mediastinum and to those particular lymph nodes. The lymph nodes are on the same side of the mediastinum as the tumor, but there was no evident metastasis. Thus, PET is more sensitive than other diagnostic techniques for detecting such metastases.

Cost-effectiveness of FDG PET in staging NSCLC

In an important paper by Verboom et al, called the PLUS study, PET was more cost-effective per patient than conventional imaging in staging NSCLC. Currently, up to 50% of the operations in

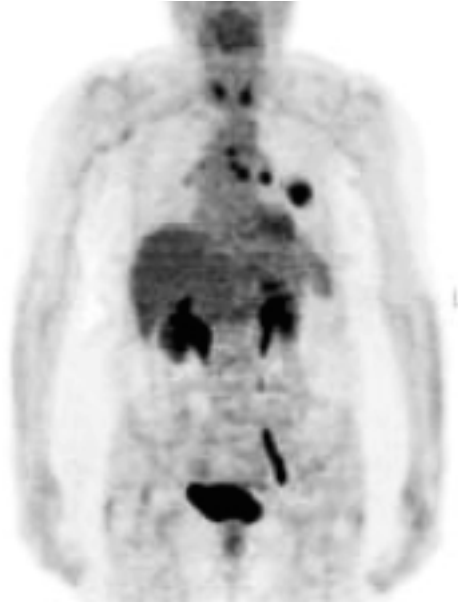


Fig. 3 PET and lung cancer: Stage IIIA (T1-3N2MO).

early NSCLC are futile owing to the presence of locally advanced tumor or distant metastases. More accurate preoperative staging is needed to reduce the number of such futile operations.

In the PLUS study, prior to invasive staging and/or thoracotomy, 188 patients with suspected NSCLC were randomly assigned to conventional work-up (CWU) and whole-body PET or to CWU alone, which was based on prevailing guidelines. Preoperative staging was followed by 1 year of follow-up. The endpoint was a futile operation as judged 1 year after surgery (i.e. metastases, disease progression).

Results

When patients were randomized to CWU with PET or without PET, 41% of operations were futile in the conventional group. However, when PET was used, that figure was cut in half to 21%. This difference was highly statistically significant ($p = 0.003$). The major cost driver was the number of hospital days related to recovery from surgery. The addition of PET to CWU prevented futile surgery in one out of five patients with suspected NSCLC.

Conclusions

Despite the additional costs for PET studies, the

total costs were lower in the PET group, mainly due to a reduction in the number of futile operations. The additional use of PET in the staging of patients with NSCLC is feasible, safe and cost-effective from a clinical and an economic perspective. Thus, PET helped to manage and guide the management of patients. This is one of many such papers that show the value of PET in cancer staging.

Quantitation of tumor uptake for NSCLC

Another important use of PET is to help quantify the uptake within the tumor. A recent paper from MSKCC evaluated the preoperative quantification of tumor uptake to predict survival after lung cancer resection in 100 consecutive patients (48 men, 52 women) with NSCLC, who had RO surgical resection and were completely free of cancer after surgery. FDG-PET was performed within 90 days before surgery. Median follow-up for surviving patients was 28 months (range, 16–81 months). An uptake measure called the standardized uptake value (SUV) was used to quantify the activity per unit volume within the tumor divided by the injected activity per body weight.

Results

Median maximal SUV (SUVmax) was 9. The 2-year survival for patients with SUVmax greater than 9 was 68% and for those with SUVmax less than 9 was 96% ($p < 0.01$).

Another predictor in this study was tumor size. In a multivariate analysis that included pathologic tumor size, involved nodes, histology, and SUVmax, only tumor size (T) greater than 3 cm and SUVmax greater than 9 and their interaction were significant predictors of survival ($p = 0.01, 0.02, \text{ and } <0.01$, respectively). The 3-year survivals for patients with both T less than 3 cm and SUVmax less than 9 was 97%; for those with T less than 3 cm and SUVmax more than 9, it was 94%; for those with T greater than 3 cm and SUVmax less than 9, it was 93%; and for those with T greater than 3 cm and SUVmax more than 9, it was 47% ($p < 0.01$).

Conclusions

SUVmax within the lesion predicts for survival in NSCLC. The addition of SUVmax to pathologic tumor size identifies a subgroup of patients at highest risk for death as a result of recurrent disease after

resection.

Not only there is information about extent of disease embedded in the PET image, but there is also information about the biology of the disease because PET imaging employs a biochemical tracer.

PET imaging to monitor treatment response

PET imaging can be used to assess tumor susceptibility as well. For example, it can be used to determine the patient's sensitivity to therapy (i.e. the presence of key molecular targets such as androgen receptor), or to assess the tumor burden. In addition, PET can be used to monitor treatment effects, such as cell-specific effects on viability (e.g. FDG SUV), effects on molecular target (e.g. DNA synthesis), and cell mass reduction. In the future, PET will be widely used to evaluate patients for treatment therapy.

Case study of a patient with lung cancer that was considered inoperable

The patient's response to radiation treatment was monitored at MSKCC using PET. The image is through the heart viewed from the back (Fig. 4). As treatment proceeded, the lesion became fainter, although it was still evident at 5,400 ray. At the end of treatment, at 6,480 CGy, some normal tissue effect was evident, but the tumor was much reduced in metabolic activity.

This response to treatment can be quantitated in different ways. Figure 5 shows a measure that actually incorporates the volume of the tumor. Over the time course of radiation treatment, this patient's

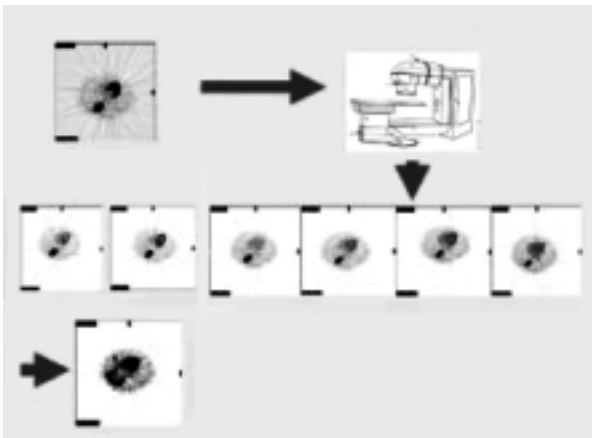


Fig. 4 Pre- and post-radiation therapy in a patient with inoperable lung.

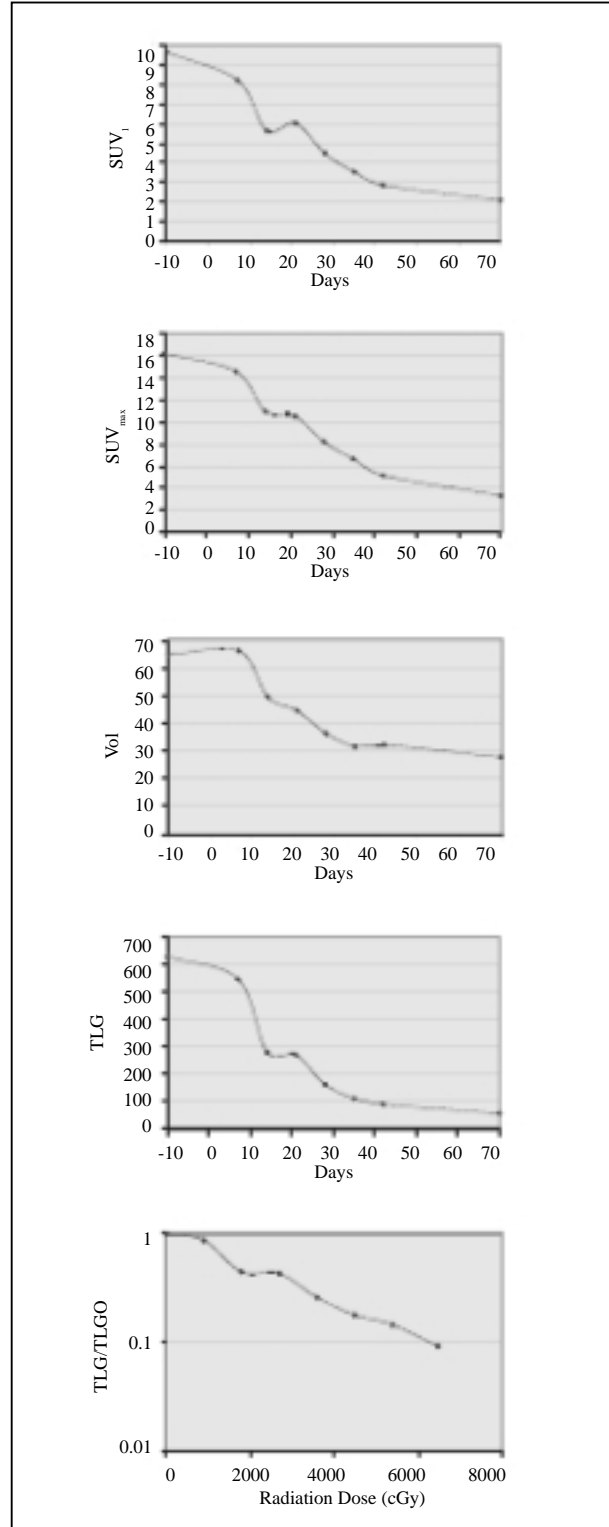


Fig. 5 Quantification of response to treatment.

tumor dropped to less than 10% of the original metabolic burden at tumor site.

Another way to represent treatment response is shown in Figure 6, in which PET data is communicated to the treatment planning computer. Sagittal images of before and after treatment show the change in the tumor.

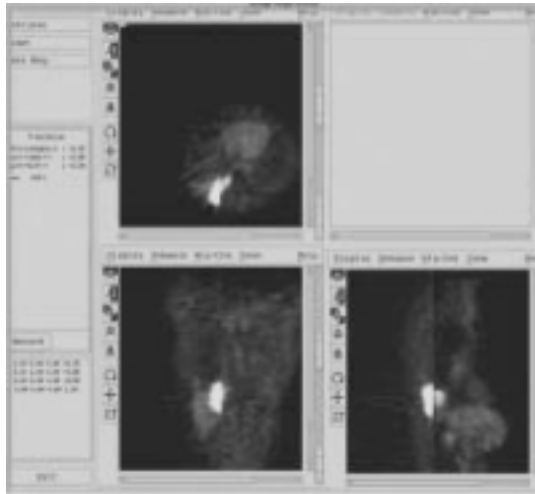


Fig. 6 Sagittal images pre - and post-radiation therapy in a patient with inoperable lung cancer.

FDG-PET uptake pattern during lung cancer

It is also important to look for changes in the patient's normal tissue because radiation will have an impact. In this patient, here were the findings: (1) baseline — mass right lung base, right hilum, left paratracheal; (2) 900 cGy — unchanged; (3) 1,800 cGy — inflammation in right posterolateral chest; (4) 2,700 cGy — intense increased FDG uptake in the esophagus — esophagitis; (5) 3,600 cGy — paratracheal uptake resolved; (6) 4,500 cGy — decreased uptake in the marrow of the lumbar spine; (7) 5,400 cGy — decreased uptake in the thoracic spine. Finding the optimal methods for displaying the actual response continues to be a challenge, and new ways to do so must be found.

PET-CT combines function and anatomy

PET-CT is a major advance because it combines function and anatomy. It can offer (1) huge attenuation correction and through-put increase — it cuts the patient's time in the camera approximately in

half; (2) real-time fusion imaging of PET-CT — there are tremendous benefits for PET positive lesions; (3) increasing the confidence that a lesion is malignant as opposed to simply a physiologic site; and (4) benefits to anatomic site of PET positive lesions. Besides, areas of special interest and importance include (1) head and neck: occult tumor; (2) bony metastases; (3) lymph node uptake; and (4) peritoneal implants versus bowel.

An excellent study in the *New England Journal of Medicine* evaluating the staging of NSCLC with PET-CT found that integrated PET-CT provided additional information in 41% (20/49) patients, beyond that provided by conventional visual correlation of PET and CT.

In this prospective study, integrated PETCT was performed in 50 patients with proven or suspected NSCLC. CT and PET alone, visually correlated PET and CT, and integrated PET-CT were evaluated separately, and a tumor-node metastasis stage was assigned on the basis of image analysis. Extrathoracic metastases were confirmed histopathologically or by at least one other imaging method.

Results

Integrated PET-CT had better diagnostic accuracy than the other imaging methods. Tumor staging was significantly more accurate with integrated PET-CT than with CT alone ($p = 0.001$), PET alone ($p < 0.001$), or visual correlation of PET and CT ($p = 0.013$). Node staging was also significantly more accurate with integrated PET-CT than with PET alone ($p = 0.013$). In metastasis staging, integrated PET-CT increased the diagnostic certainty in two out of eight patients.

Conclusions

Tumor staging is more accurate with PET-CT than with CT alone or with PET alone. This is the kind of information that gives one confidence about the site of the lesion and also about the staging.

Respiratory gating of PET images

The greatest source of error in accurate localization and quantification on PET and PET/CT of tumors in lung cancer is respiratory motion. There is a significant swing, in small tumors especially and at the base of the lungs, which blurs the image. It spreads the count and radioactivity over a larger vol-

ume and thus reduces the number of counts in a particular region.

In the Nuclear Medicine department at MSKCC, a physics team of about five people works on medical problems related to nuclear medicine. This group has published several papers relating to respiratory gating in PET-CT. Respiratory-gated PET is used in treatment planning by means of a camera-based unit that monitors the respiratory excursion through a reflector system. The approach is similar to what has been done with gating of cardiac studies in nuclear medicine. Data are collected according to a physiologic signal. A collection of data is triggered in temporal bins related to the physiologic trigger. When the patient takes a breath and it swings up to a peak, the counts are entered in that bin. When the patient exhales and it drops, the counts are entered in that bin. There is also a bin for interbreaths.

Nehmeh et al reported on the variability of respiratory motion during 4D-PET-CT acquisition for five lung cancer patients who were monitored by tracking external markers placed on the abdomen. CT acquisition of the lesion occurs in seconds, rather than the 4–6 minutes required for PET scans. As a result, an incongruent lesion position during CT acquisition will bias activity estimates using PET.

Methods

CT data were acquired over an entire respiratory cycle at each couch position. The X-ray tube status was recorded by the tracking system, for retrospective sorting of the CT data as a function of respiration phase. Each respiratory cycle was sampled in 10 equal bins. 4D-PET data were acquired in gated mode, where each breathing cycle was divided into 10,500 ms bins. For both CT and PET acquisition, patients received audio prompting to regularize breathing. The 4D-CT and 4D-PET data were then correlated according to their respiratory phases. The respiratory periods and average amplitude within each phase bin, acquired in both modality sessions, were then analyzed.

Results

The average respiratory motion period during 4DCT was within 18% of that in the 4D-PET sessions.

This would reflect up to 1.8% fluctuation in the duration of each 4D-CT bin. This small uncertainty

enabled good correlation between CT and PET data, on a phase-to-phase basis. Comparison of the average amplitude within the respiration trace, between 4D-CT and 4D-PET, on a bin-by-bin basis showed a maximum deviation of approximately 15%.

Conclusions

This study proved the feasibility of performing 4D-PET-CT acquisition. Respiratory motion was in most cases consistent between PET and CT sessions, thereby improving both the attenuation correction of PET images and co-registration of PET and CT images.

Figure 7 illustrates the difference between gated and ungated images in the region of the tumor. There is a change in the tumor appearance depending on the bin. Some distortion occurs with the tumor that can be quite profound. The lesion in the gated image is smaller in diameter than in the ungated image and also exhibits a change in shape. Therefore, it is highly desirable to control the shape in order to better detect the radioactivity in the lesion as well as to plan for a radiotherapy target volume. Sometimes normal tissue must be irradiated to guarantee that the whole region (nongated) is being irradiated.

In a follow-up study, Erdi et al. systematically analyzed the range of activity concentration changes, i.e. SUV, for eight lung lesions in the five lung cancer patients scanned with PET-CT.

Methods

In CT, data were acquired in correlation with the real-time positioning system. PET data were acquired after intravenous injection of about 444–555 MBq of ^{18}F -FDG with a 1-hour uptake period. The scanning time was 3 minutes per bed posi-

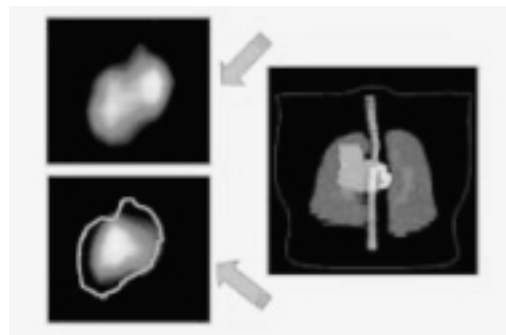


Fig. 7 Gated versus non-gated PET: Treatment planning. 11
Reproduced with permission from the source.

tion for PET. CT images were sorted into 10 phases, with 0% corresponding to end of inspiration (EI) and 50% corresponding to end of expiration (EE).

Using the respiration-correlated CT data, images were re-binned to match the PET slice locations and thicknesses.

Results

The gated images showed a significant reduction in the apparent volume of the lesions (Fig. 8).

Reconstructed PET emission data showed up to a 24% variation in the lesion SUVmax between EI and EE phases. Examination of all the phases showed an SUV variation of up to 30%. Also, in some cases the lesion showed up to a 9 mm shift in location and up to a 21% reduction in size when measured from PET during the EI phase, compared with the EE phase.

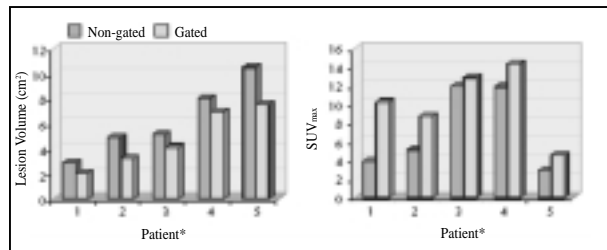


Fig. 8 Gated PET effects: Lesion volume and SUVmax. Reproduced with permission from the source.

Conclusions

Using respiration-correlated CT for attenuation correction, the fluctuations in PET SUVs could be quantified. Because those changes may lead to estimates of lower SUVs, the respiratory phase during CT scanning needs to be measured or lung motion has to be regulated for imaging lung cancer in routine clinical practice.

Drs Nehmeh and Erdi working under the leadership of Dr Humm, in conjunction with engineers from the GE Medical Systems, have begun to refine this technique to evaluate the effect of respiratory gating on pulmonary lesions. They first tested a technique referred to as respiratory-correlated dynamic PET (RCDPET) by comparing it with respiratory-gated PET (RGPET). RCDPET enables the acquisition of 4-dimensional PET (4D-PET) data without

the need for a respiratory tracking device. Both RCDPET and RGPET provide the ability to correct for motion artifacts and more accurately quantify radiotracer uptake within lung lesions. Both methods were evaluated in phantom studies and one patient.

Methods

With RCDPET, data were acquired in consecutive 1-second time frames. A point source attached to a rigid foam block was set on the patient's abdomen and was extended into the camera field of view at the level of the lesion by means of a low-density rod. The position of this source was used to track respiratory motion through the consecutive dynamic frames. Image frames corresponding to a user-selected lesion position within the breathing cycle, in correlation with the point source position, were then identified after scanning. The sinograms of the selected image frames were summed and then reconstructed using iterative reconstruction with segmented attenuation correction.

Results

Phantom studies of both RGPET and RCDPET were within 10% agreement, for both activity quantitation and image noise levels. In a clinical application, the quantitation of the SUVmax and the size of the lesion showed differences of 6% and 2%, respectively, between RCDPET and RGPET measurements.

Conclusions

RCDPET can be considered a comparable or alternative method to RGPET in reducing the smearing effects due to respiration and improving quantitation of PET in the thorax. One advantage of RCDPET over RGPET is the ability to retrospectively reconstruct the PET data at any phase or amplitude in the breathing cycle.

Extending these findings to respiratory-correlated acquisition on PET-CT, Nehmeh, Erdi, et al. evaluated PET imaging of lung lesions on PET-CT through RCDPET. The objectives of the study were: (1) to correct for respiratory motion artifacts in PET imaging; and (2) to match PET and CT phases for the purpose of improving the local co-registration of PET and CT and to more accurately quantitate the lesion SUV.

4D-CT acquisition uses a step-and-shoot tech-

nique of (1) axial FOV of 10 mm (four 2.5 mm slices); (2) scan time of (T+1) sec, typically (5+1) sec; (3) tube speed, X-ray of per Rotation/0.5 sec; (4) time interval between images of 0.45 sec.

With 4D-PET-CT fusion, a particular time in the respiratory cycle and the same time in the CT respiratory cycle are selected, and the images are then fused simultaneously. Figures 9 and 10 compare images with RC-CT with 4-D-PET-CT fusion.

The result is very accurate local co-registration that can then be used to make an attenuation correction and obtain an SUV or other quantification measure. Figure 11 compares RCDPET with 4D-PET-CT to illustrate differences in the appearance of the tumor mass. The latter images are much more sharply defined with better borders. Gating gives a much clearer picture resulting in more than a one-third increase in the quantification. This kind of image provides very valuable treatment planning

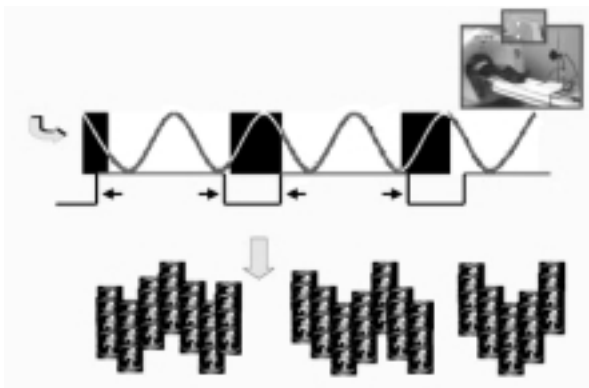


Fig. 9 Respiratory-correlated CT. 6 Reproduced with permission from the source.

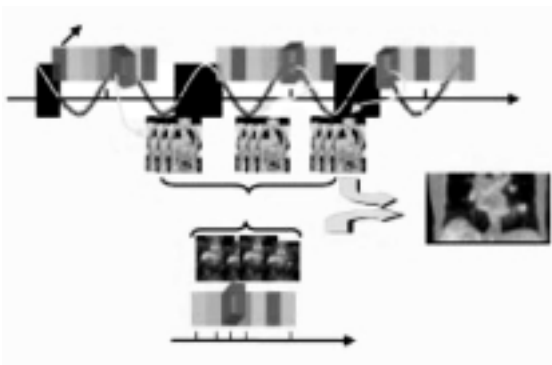


Fig. 10 4D-PET-CT fusion. 6 Reproduced with permission from the source.

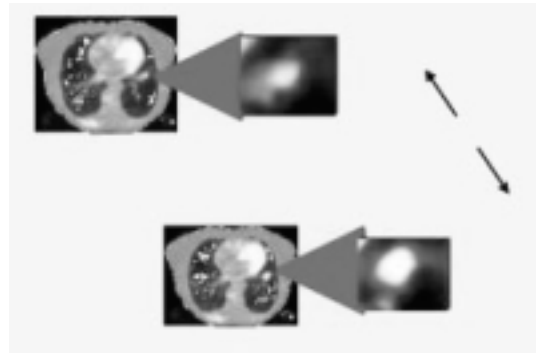


Fig. 11 Improved local co-registration: Gated PET versus gated PET with 4D-CT-AC.9 Reproduced with permission from the source.

information. However, it is a challenge in terms of intense computation.

What's next?

With the availability of CT, which can provide more accurate quantitation of motion and of the attenuation map, significant statistical data are needed to evaluate the correlation between the motion and the change in the SUV between the gated and nongated measurements. The SUV of lung lesions must be re-evaluated based on 4D-PET-CT acquisition. In addition, discrepancies must be re-evaluated between Ge-68 AC and CT-AC for all organs affected by respiration. This development will have important implications in areas such as the liver for controlling respiratory motion, which is a major problem in terms of lesion detection. Work in that area is just underway.

Automated lesion definition

In a collaborative effort between MSKCC and the GE Global Research Center, Sebastian et al. inserted artificial lesions (based on patient datasets) into normal scans as 'round truth' from 35 patients with 278 lesions. Different locations near the organs were chosen, ranging in size from 5 to 40 cc with various levels of SUVs (3.1–7.1). This was used as ground truth from which segmentation algorithms, based on a directionally dependent model of the background, were developed. The segmented tumor volume (V_s) and the embedded tumor volume (V_{gt}) were compared using the percent true positive and false positive volumes (Table).

This technique can be applied to automate

lesions to help in the segmentation of tumor volume.

It may also aid us in evaluating tumor mass and the effect of tumor burden on patient response.

Until now, this parameter for treatment response has not received much attention because it has been too difficult to evaluate. Automated methodologies, however, should allow us to make that kind of assessment. This program is now available on the GE Advantage workstation at several institutions.

Table. Performance Metrics for Tumour Segmentation

Volume	5 cc	10 cc	25 cc	40 cc
% TPV	92.5 ± 8.5	93.6 ± 7.5	93.9 ± 6.2	92.4 ± 3.2
% FPV	39.7 ± 16.9	31.0 ± 11.2	27.8 ± 8.8	22.8 ± 10.9

% TPV = 100*(Vgt^Vs)/Vgt; % FPV = 100*(Vgt - Vs)/Vgt.

Summary and conclusion

We have successfully taken the first step toward 4D-PET-CT acquisition, in an attempt to correct for respiratory motion artifacts in PET imaging of lung lesions. 4D-PET-CT imaging results in improved local co-registration and quantitation (SUV).

REFERENCES

1. Verboom P, van Tinteren H, Hoekstra OS, PLUS study group, et al. Cost-effectiveness of FDG-PET in staging non-small cell lung cancer: the PLUS study. *Eur J Nucl Med Mol Imag* 2003;30:1444–9. Epub 2003 May 29.
2. Downey RJ, Akhurst T, Gonen M, et al. Preoperative F-18

fluorodeoxyglucose-positron emission tomography maximal standardized uptake value predicts survival after lung cancer resection. *J Clin Oncol* 2004;22:3255–60.

3. Lardinois D, Weder W, Hany TF, et al. Staging of non-small-cell lung cancer with integrated positron-emission tomography and computed tomography. *N Engl J Med* 2003;348:2500–7.
4. Nehmeh SA, Erdi YE, Pan T, et al. Quantitation of respiratory motion during 4D-PET/CT acquisition. *Med Phys* 2004;31:1333–8.
5. Erdi YE, Nehmeh SA, Pan T, et al. The CT motion quantitation of lung lesions and its impact on PET-measured SUVs. *J Nucl Med* 2004;45:1287–92.
6. Nehmeh SA, Erdi YE, Rosenzweig KE, et al. Reduction of respiratory motion artifacts in PET imaging of lung cancer by respiratory correlated dynamic PET: methodology and comparison with respiratory gated PET. *J Nucl Med* 2003;44:1644–8.
7. Nehmeh SA, Erdi YE, Pan T, et al. Quantitation of respiratory motion during 4D-PET/CT acquisition. *Med Phys* 2004;31:1333–8.
8. Sebastian BRM, Manjeshwar RM, Akhurst TA. Evaluation of a segmentation algorithm for tumors in F-18 positron emission tomography images. June 21st, 2004 SNM 51st Annual Meeting, Philadelphia. *J Nucl Med*, Abstract #208.
9. Nehmeh SA, Erdi YE, Pan T, et al. Four-dimensional (4D) imaging of the thorax. *Med Phys* 2004;31:3179–86.
10. Erdi YE, Macapinlac H, Rosenzweig KE, et al. Use of PET to monitor the response of lung cancer to radiation treatment. *Eur J Nucl Med* 2000;27:861–6.
11. Nehmeh SA, Erdi YE, Ling CC, Rosenzweig KE, Schoder H, Larson SM, Macapinlac HA, Squire OD, and Humm JL. Effect of respiratory gating on quantifying PET images of lung cancer. *J Nucl Med* 2002;43:876–81.